Distinctive Picosecond Spin Polarization Dynamics in Bulk Half Metals

M. Battiato, J. Minár, W. Wang, W. Ndiaye, M. C Richter, O. Heckmann, J.-M Mariot, F. Parmigiani, K. Hricovini, C. Cacho

Distinctive Picosecond Spin Polarization Dynamics in Bulk Half-Metals

M. Battiato,[1,2] J. Minár,[3] W. Wang,[4] W. Ndiaye,[5] M. C. Richter,[5,6] O. Heckmann,[5,6]
J.-M. Mariot,[7,8] F. Parmigiani,[9,10,11] K. Hricovini,[5,6] and C. Cacho[12,13]

[1]*School of Physical and Mathematical Sciences, Physics and Applied Physics, Nanyang Technological University, 21 Nanyang Link, Singapore, Singapore*
[2]*Institute of Solid State Physics, Technische Universität Wien, Wiedner Hauptstraße 8, 1040 Vienna, Austria*
[3]*New Technologies-Research Center, University of West Bohemia, Univerzitni 8, 306 14 Pilsen, Czech Republic*
[4]*Department of Physics, Biology and Chemistry, Linköping University, 581 83 Linköping, Sweden*
[5]*Laboratoire de Physique des Matériaux et des Surfaces, Université de Cergy-Pontoise, 5 mail Gay-Lussac, 95031 Cergy-Pontoise, France*
[6]*DRF, IRAMIS, SPEC – CNRS/UMR 3680, Bât. 772, L'Orme des Merisiers, CEA Saclay, 91191 Gif-sur-Yvette Cedex, France*
[7]*Sorbonne Université, CNRS (UMR 7614), Laboratoire de Chimie Physique–Matière et Rayonnement, 4 place Jussieu, 75252 Paris Cedex 05, France*
[8]*Synchrotron SOLEIL, L'Orme des Merisiers, Saint-Aubin, BP 48, 91192 Gif-sur-Yvette, France*
[9]*Dipartimento di Fisica, Università degli Studi di Trieste, via A. Valerio 2, 34127 Trieste, Italy*
[10]*Elettra-Sincrotrone Trieste S.C.p.A., Strada Statale 14, km 163.5, 34149 Basovizza, Italy*
[11]*International Faculty, Universität zu Köln, 50937 Köln, Germany*
[12]*Diamond Light Source, Harwell Science and Innovation Campus, Didcot OX11 0DE, United Kingdom*
[13]*Central Laser Facility, Rutherford Appleton Laboratory, Didcot OX11 0QX, United Kingdom*

(Dated: July 27, 2018)

Femtosecond laser excitations in half-metal (HM) compounds are theoretically predicted to induce an exotic picosecond spin dynamics. In particular, conversely to what is observed in conventional metals and semiconductors, the thermalization process in HMs leads to a long living partially thermalized configuration characterized by three Fermi–Dirac distributions for the minority, majority conduction, and majority valence electrons respectively. Remarkably, these distributions have the same temperature but different chemical potentials. This unusual thermodynamic state is causing a persistent non-equilibrium spin polarization only well above the Fermi energy. Femtosecond spin dynamics experiments performed on Fe_3O_4 by time- and spin-resolved photoelectron spectroscopy are support on our model. Furthermore, the spin polarization response proves to be very robust and it can be adopted to selectively test the bulk HM character in a wide range of compounds.

Ultrafast magnetization dynamics covers a wide range of scientifically advanced and technologically attractive phenomena ranging from ultrafast demagnetization [1] to spin transport [2–6], all-optical switching [7], antiferromagnet spin dynamics [8], and artificial ferrimagnets [9]. This scenario has fostered a significant effort for studying the magnetization dynamics and the distinctive interplay between the metallic and the insulating spin channels in half-metals (HMs), such as Heusler compounds and oxides (see, e.g., Refs. [10–12]). This exotic dependence of the transport properties on the spin channels makes the physics of the HMs puzzling and striking [13, 14].

Typically, HMs show a relatively slow demagnetization, i.e., few tenths of picoseconds, supposed to be governed by the slow spin-lattice channel as the Elliot–Yafet spin-flip scattering is blocked in the gapped energy region [15, 16]. However, a fast demagnetization was reported in $Co_2Mn_{1-x}Fe_xSi$ and a fast spin-flip scattering path, in connection with the valence band photohole below the Fermi level (E_F), was invoked to explain such a finding [17–19]. Therefore, it remains unclear if and what kind of distinctive ultrafast electronic mechanisms should be expected in HMs, beyond the material dependent electron-phonon coupling.

To address this challenge we have studied theoretically the ultrafast thermalization dynamics in HMs by solving the time-dependent Boltzmann scattering equation. A thermalization dynamics characterized by a long lasting partially equilibrated electronic distribution was identified. This dynamics shows peculiarities clearly discriminating the HMs from ordinary metals and semiconductors. In particular, a novel transient high energy spin polarization (SP) is found and its dynamics can be easily distinguished from other magnetization dynamics triggered by independent mechanisms such as ultrafast demagnetization [1, 20], ultrafast spin transport [2, 5, 6], or increase in magnetization [3, 21]. Femtosecond spin dynamics experiments performed on Fe_3O_4 by time- and spin-resolved photoemission (PE) have successfully benchmarked the physics of our model. The experiments reported here unlock the gate for unambiguously testing the bulk half metallicity (HMy).

A wide range of techniques has been put forward to verify HMy, however they can be made complicated for a number of reasons. For instance, the results of ferromagnetic-superconducting tunneling measurements can be strongly affected by hard-to-predict properties of the reconstructed surfaces and interfaces [22]. This is also the case for Andreev reflection measurements in which the extraction of quantitative information relies on

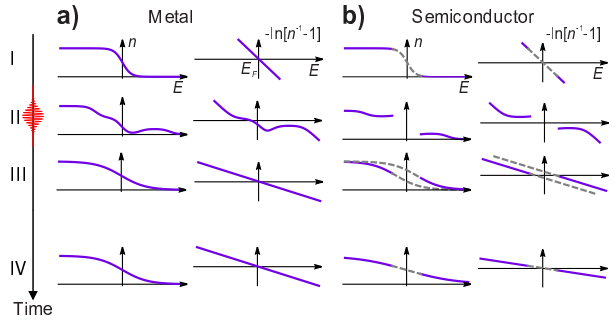

FIG. 1. (Color online) Electron distribution function n during the thermalization following a femtosecond laser excitation in a metal (a) and a semiconductor (b). Both linear (left column) and logarithmic (right column) representations are plotted to highlight the location of E_{F} and the electronic temperature (see text for details).

the way scattering at contacts is dealt with [23]. Transient magneto-optical Kerr effect measurements [16] do not show a universal response for all HMs [17–19]. Spin- and angle-resolved PE [24] is the most direct experimental method to test HMy (see, e.g., Ref. [25]). Nevertheless its high surface sensitivity can raise difficulties when bulk properties are concerned (for a discussion of this issue in the case of Fe_3O_4, see Ref. [26]). A further problem arises from the presence of polarons which strongly modifies the spectral weight at E_{F}, hampering a direct comparison of the experimental data to state-of-the-art calculations of the PE spectra [27]. In this context identifying a clear fingerprint of bulk HMy remains an open challenge.

It is well known that electron-hole pairs created in metals under light excitation quickly decay via electron-electron scattering and form lower energy electrons and holes close to E_{F}, until a Fermi–Dirac (FD) distribution with a higher temperature is formed. Figure 1(a) schematically illustrates the time (t) evolution (from top to bottom) of the electron distribution n depending on the energy (E) in a metal after a femtosecond laser excitation. The initial FD distribution (I) evolves into a non-equilibrium distribution (II) after the laser pulse, and then, via thermalization, into another FD distribution characterized by a higher temperature (IV). A more enlightening representation of the time dependence is given in the second column of Fig. 1(a) using the $-\ln\left(n^{-1}-1\right)$ function, as proposed in Ref. [28], that is, for a FD distribution, linear in E with a slope $\propto -1/k_{\mathrm{B}}T$ and a zero crossing at the chemical potential energy [see Fig. 1(a) panels I, III, and IV of the second column]. A non-linear behavior is associated to non-thermal distributions.

In a semiconductor, the thermalization process is completely different [Fig. 1(b)]. The initial FD distribution (I) is strongly modified by the laser pulse (II) but, contrary to the metallic situation, the thermalization occurs in two steps. First electron-electron and electron-phonon scattering brings the excited electrons (hole) close to the top (bottom) of the conduction (valence) band (III). This intermediate state is a partially equilibrated state, characterized by two FD distributions with the same temperature but different chemical potentials for the electrons and the holes [notice in (III) the different zero crossing of the two linear branches of $-\ln\left(n^{-1}-1\right)$]. It is only on a longer timescale that a full electron-hole recombination takes place.

In a HM, where one of the spin channel is metallic and the other insulating, it is far from clear what is happening because both channels will not behave as simply as two non-interacting populations as, even in the absence of spin-flip transitions, electrons belonging to one spin channel can scatter with the electrons of the other one.

To answer this question, we solve numerically the time-dependent Boltzmann equation for electron-electron scattering in a spin-dependent density of states (DOS) ρ after a laser excitation. The time dependence of the electron distribution $n(\sigma, E, t)$ within the spin(σ)- and energy(E)-dependent DOS $\rho(\sigma, E)$ is calculated [2, 4] as

$$\begin{aligned}\frac{\partial n}{\partial t} = & S_{\mathrm{exc}} \\ & - \alpha \sum_{\sigma''} \int n\, \rho'(1-n')\, \rho'' n''\, \rho'''(1-n''')\, \mathrm{d}E'\, \mathrm{d}E'' \\ & + \alpha \sum_{\sigma''} \int (1-n)\, \rho' n'\, \rho'' n''\, \rho''''(1-n'''')\, \mathrm{d}E'\, \mathrm{d}E''\end{aligned} \tag{1}$$

where $n = n(\sigma, E, t)$, $n' = n'(\sigma, E', t)$, $n'' = n(\sigma'', E'', t)$, $n''' = n(\sigma'', E + E'' - E', t)$, and $n'''' = n(\sigma'', E' + E'' - E, t)$, and the same convention for ρ. The laser excitation is within the term $S_{\mathrm{exc}} = S_{\mathrm{exc}}(\sigma, E, t)$ and depends on the pump pulse parameters (duration, photon energy and intensity). Notice how electrons with different spins can scatter with each other but the total spin is preserved. Spin-flip scatterings are ignored due to their small number. We will address below how the dynamics is affected when these scatterings are included. The scattering amplitude α is kept as a constant parameter. The lack of energy and spin dependence of α is, for our purpose, an excellent approximation as the dynamics is overwhelmingly dictated by the size of the scattering phase space (i.e., the number of spin and energy conserving scatterings).

For the bulk Boltzmann scattering calculations we use the Fe_3O_4 spin-resolved DOS computed from first principles using the SPR-KKR package [29] based on the Korringa–Kohn–Rostoker method and the Dirac equation, to take into account all relativistic effects. To treat the correlated $3d$ states of Fe, the local spin-density approximation+U method was used. The corresponding bulk DOS for $U = 2.0\,\mathrm{eV}$ and $J = 0.9\,\mathrm{eV}$, shown in the top panels of Fig. 2(a and b), are in very good agreement with previous theoretical results [30, 31]. The layered resolved DOS of $Fe_3O_4(1\,0\,0)$ reconstructed surface from

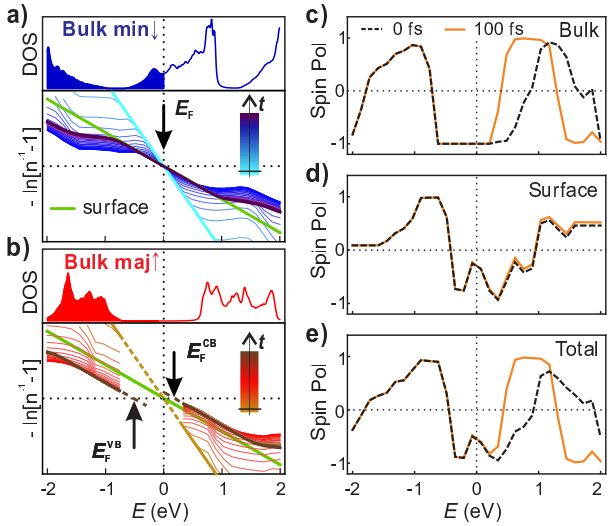

FIG. 2. (Color online) Electron thermalization after a laser pulse excitation in Fe_3O_4: (a) Time evolution (up to 200 fs) of the electron distribution n in the $-\ln\left(n^{-1}-1\right)$ representation for the metallic minority spin channel (bottom panel). The top panel shows the corresponding DOS of bulk Fe_3O_4. (b) Same for the insulating majority spin channel showing the presence of two chemical potentials. Using the metallic surface DOS, the calculations converge toward the solid green line with a single chemical potential. (c–e) Time dependence of the SP calculated for the bulk (HM), the surface (metal), and for a 50:50 mixture of bulk and surface contributions, respectively.

Ref. [31] was used to take into account the (metallic) surface dynamics in solving the Boltzmann equation.

The time evolution of the electron distribution in the vicinity of E_F for the bulk minority spin (metallic channel) is presented in Fig. 2(a). Starting from a room temperature FD distribution (cyan line), the population evolves via a non-thermal distribution to a partially-thermalized distribution (from light to dark blue lines) and eventually reaches a fully thermalized population. A similar calculation performed for the metallic surface leads to a fully thermalized distribution (green line). The existence of partial thermalization can be observed at very high and very low energies [i.e., the function $-\ln\left(n^{-1}-1\right)$ is not a straight line]. It is due to the presence of the two regions with very low electronic densities, which act as effective band gaps. We mention this point for the sake of completeness but it is not relevant to and does not affect the conclusions of this work.

More interesting is the dynamics in the majority spin gapped channel [Fig. 2(b)]. Here the initial population evolves toward two FD-like distributions with distinct chemical potential located (see the black arrows at zero crossing) in the valence and conduction bands (VB and CB) and with the same electronic temperature (same slope in the logarithmic representation). This result is a direct consequence of the lack of empty final states around E_F available to allow relaxation of the CB electrons and it closely resembles the behavior of an isolated semiconducting system. Hereafter we will refer to this non-equilibrium state as the partial thermalization. Due to the slow recombination of electron-hole pairs in this channel, this partially thermalized distribution persists for a long time (dark brown line). The full thermal equilibrium is reached only on a timescale that largely exceeds the computed timescale (not shown in the figure).

Such spin-asymmetric thermalization leads to the unusual situation where the SP of the partially thermalized hot carrier is strongly different from the DOS SP. The SP [Fig. 2(c)] at the thermal equilibrium (dashed line) is the SP of the DOS (the PE matrix element effects are ignored here). After the laser excitation and an initial partial thermalization process, the accumulation of majority carriers at the bottom of the CB leads to an increase of SP in the energy range above 0.5 eV. Due to the very slow nature of the second part of the thermalization process this out-of-equilibrium polarization persists for a long time (black line). It is here important to notice that no change in the SP is observed around the equilibrium E_F and below.

The above outlined SP dynamics is uniquely characteristic of HMy. Furthermore, it can be observed even in the presence of a metallic sample surface because, then, the carriers in both spin channels quickly decay to energies close to E_F. The surface SP briefly changes during the non-thermal regime due to the spin dependent laser excitation. However, within a few tens of femtosecond, the electron-electron scattering leads to a thermal equilibrium between both spin channels with a single FD distribution and the SP (black line) returns quickly to the equilibrium SP [see the dashed line in Fig. 2(d)]. In Fig. 2(e) we plot the superimposed spin dynamics of surface and bulk (i.e., 50:50 mixture) that shows how the bulk HMy effect (i.e., SP increase at high energies) is very resilient to the presence of the metallic surface. The effect is also resilient to spin-flip processes or transport between bulk and surface that would contribute only to reduce the survival time of the out-of-equilibrium SP, but not prevent its appearance. Other effects, like polarons, that broaden the spectrum cannot mask this effect either.

It is also fundamental to appreciate how this peculiar spin dynamics (increase of SP only well above E_F) is qualitatively different from what one would observe in other types of magnetization dynamics, where the change of SP is expected either around E_F or at all energies [1–3, 5, 6, 20, 21]. Finally this dynamics cannot be confused with the one triggered by spin-asymmetric optical excitation (observed in our surface calculations) since that one survives for just a few tens of femtosecond.

We now apply our strategy to Fe_3O_4, the HMy of which is acknowledged to be difficult to measure due to its metallic surface and polaronic broadening of the PE spectra. A time-, energy-, and spin-resolved PE ex-

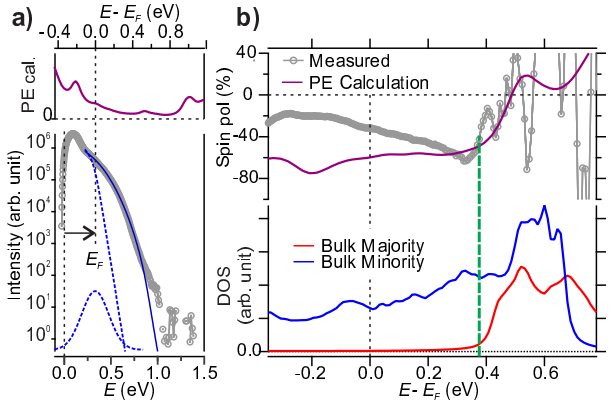

FIG. 3. (Color online) Photoemission from Fe_3O_4. (a) The Fe $3d(t_{2g})$ EDC at 4.65 eV photon energy (lower panel, log scale, grey dots) is fitted (solid blue line) by a function including the one-step PE calculation (top panel), a FD distribution, and a broadening function (blue dashed lines). (b) Both measured and calculated SP (top panel) are referenced to the bulk DOS (lower panel) indicating the position (vertical green line) of the bottom of the CB.

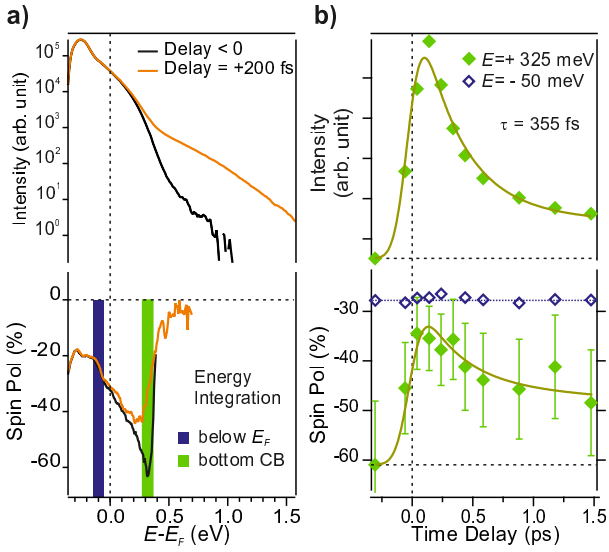

FIG. 4. (Color online) Spin dynamics in Fe_3O_4 above E_F. (a) Spin-integrated EDC (top panel) before (black line) and 200 fs after (orange line) pump excitation. The corresponding SP (bottom panel) increases at the bottom of the CB (green bar) as theoretically predicted for a HM. (b) The dynamics of the hot carriers (top panel) at this energy is well described by an exponential decay function characteristic of an electron-phonon cooling. The SP (bottom panel) relaxes on a similar time scale whereas the SP below E_F (empty blue diamond), proportional to the macroscopic magnetization, remains unchanged.

periment was carried out by combining a 250 kHz repetition rate Ti:sapphire laser source with a homebuilt electron time-of-flight spin analyzer [32]. The third harmonic (4.65 eV) of the fundamental beam was generated by frequency mixing in β-barium borate crystals. For the pump beam at 1.55 eV photon energy, 10% of the laser source was delayed and focused on the sample, giving a maximum fluence of 0.7 mJ cm^{-2}. Both pump and probe were p-polarized and the overall time resolution of the experiment was 150 fs. A $\approx$ 50 nm thick Fe_3O_4(0 0 1) film was epitaxially grown on MgO(1 0 0) under ultra-high vacuum and characterized by low-energy electron diffraction (LEED), x-ray magnetic circular dichroism, and x-ray photoelectron spectroscopy. The LEED pattern showed a clear $(\sqrt{2} \times \sqrt{2})$R45° surface reconstruction.

The use of 4.65 eV photons gives access to electrons in the vicinity of E_F only, as observed on the energy distribution curve (EDC) at normal emission [Fig. 3(a) (lower panel, log scale, grey dots)]. The Fe $3d(t_{2g})$ spectral weight at E_F does not show the sharp edge expected for a metal as it is smeared out by strong polaronic effects and initial state lifetime broadening [27, 33, 34].

The experimental EDC is very well reproduced, over three orders of magnitude (solid blue line), by the convolution of the calculated PE [35–37] with a 330 meV FWHM Gaussian function (dash blue lines), accounting for the polaronic effects [27] and a FD distribution. Only the E_F position and the Gaussian width are free parameters in the fitting procedure. Due to the majority bulk band gap, the measured SP is negative around E_F and reaches only a −65 % minimum at 360 meV above E_F [Fig. 3(b) (top panel)] due to the metallicity of the surface. The *ab initio* calculations overestimate the SP, an effect that we attribute to the surface reconstruction, not accounted for in our calculations.

Next we investigate the electron spin dynamics above E_F after optical excitation. In Fig. 4(a) the EDCs (top panel) at negative delay and at +200 fs delay (maximum excited electron population) are compared. A clear presence of excited electrons is detected up to +1.5 eV above E_F. The SP below E_F (bottom panel) remains unchanged whereas, very interestingly, a clear reduction of the SP is observed in the energy region +360 meV, corresponding to the bottom of the majority spin bulk CB. The time evolution of this population [Fig. 4(b) (top panel, solid line)] is fitted by an exponential decay function (time constant of 355 fs) plus a constant offset (to account for the extremely slow dynamics). After excitation the population relaxes quickly via a number of mechanisms such as electron-electron and electron-phonon scattering. However a large number of carriers remains trapped at the bottom of the bulk majority spin CB, and survive at high energy for a long time ($t > 1.5$ ps). The time evolution of the SP [Fig. 4(b) (bottom panel)] shows a similar behavior and has been fitted with the same time relaxation as for the intensity. During and shortly after the laser excitation a non trivial SP dynamics is activated. Interestingly after 1.5 ps the

SP does not relax back to the equilibrium value, as one would expect if the electronic system was fully thermalized. It remains $\approx 25\%$ higher than its equilibrium value, giving evidence of the presence of a non fully thermalized population persisting in time. As this delay is much longer than the typical electron-electron scattering time we can safely attribute this population to the partially thermalized state described in our model where a transient chemical potential is localized only in the majority spin CB. To assess any possible ultra-fast demagnetization contribution in our SP dynamics we present the SP measured below E_{F} in Fig. 4(b) (empty diamond). The fact that it remains constant over time confirms that the magnetite retains its full magnetization during our time window.

The above dynamics is in striking qualitative agreement with the theoretical picture we have presented. The accumulation of carriers at a finite energy above E_{F} shows the presence of a bandgap, while the transient SP allows for the identification of the spin channel where the gap is located, despite a number of details are unknown, like structural and chemical reconstruction of the surface. This proves that a non-equilibrium SP at high energy, persisting well after any short-lived SP dynamics close to E_{F} has ended, is a reliable and resilient fingerprint of HMy.

In summary, we have modeled the electron thermalization following a femtosecond laser pulse in Fe_3O_4 by solving the time dependent Boltzmann scattering equation. The bulk population dynamics is found to be characterized by the formation of a persisting partial thermalization, where majority carriers remain trapped at the bottom of the CB. The long lasting out-of-equilibrium distribution in the CB leads to an increase of the SP well above E_{F} despite the metallic nature of the surface. The agreement between experiments and theory shows that this peculiar fingerprint in the picosecond SP dynamics can be used to probe bulk HMy. Extension of the work to other examples is certainly needed but our contribution is intended to spur long-term and far-reaching actions in line with the efforts made worldwide to understand the spin dynamics in condensed matter.

The electron ToF-Spin analyzer was funded by a UK EPSRC grant (GR/M50447) and supported by STFC, and the FERMI FEL project (Elettra). M.B. gratefully acknowledges the Austrian Science Fund (FWF) through Lise Meitner position M1925-N28 and Nanyang Technological University, NAP-SUG for the funding of this research. J.M. was supported by the project CEDAMNF, reg. no. CZ 02.1.01/0.0/0.0/15_003/0000358, co-funded by the ERDF.

[1] E. Beaurepaire, J.-C. Merle, A. Daunois, and J.-Y. Bigot, "Ultrafast spin dynamics in ferromagnetic nickel," Phys. Rev. Lett. **76**, 4250 (1996).

[2] M. Battiato, K. Carva, and P. M. Oppeneer, "Superdiffusive spin transport as a mechanism of ultrafast demagnetization," Phys. Rev. Lett. **105**, 027203 (2010).

[3] D. Rudolf, C. La-O-Vorakiat, M. Battiato, R. Adam, J. M. Shaw, E. Turgut, P. Maldonado, S. Mathias, P. Grychtol, and H. T. Nembach *et al.*, "Ultrafast magnetization enhancement in metallic multilayers driven by superdiffusive spin current," Nat. Commun. **3**, 1037 (2012).

[4] M. Battiato, K. Carva, and P. M. Oppeneer, "Theory of laser-induced ultrafast superdiffusive spin transport in layered heterostructures," Phys. Rev. B **86**, 024404 (2012).

[5] M. Battiato, P. Maldonado, and P. M. Oppeneer, "Treating the effect of interface reflections on superdiffusive spin transport in multilayer samples (invited)," J. Appl. Phys **115**, 172611 (2014).

[6] M. Battiato and K. Held, "Ultrafast and gigantic spin injection in semiconductors," Phys. Rev. Lett. **116**, 196601 (2016).

[7] C. D. Stanciu, F. Hansteen, A. V. Kimel, A. Kirilyuk, A. Tsukamoto, A. Itoh, and Th. Rasing, "All-optical magnetic recording with circularly polarized light," Phys. Rev. Lett. **99**, 047601 (2007).

[8] A. V. Kimel, A. Kirilyuk, A. Tsvetkov, R. V. Pisarev, and Th. Rasing, "Laser-induced ultrafast spin reorientation in the antiferromagnet $TmFeO_3$," Nature **429**, 850 (2004).

[9] S. Mangin, M. Gottwald, C.-H. Lambert, D. Steil, V. Uhlíř, L. Pang, M. Hehn, S. Alebrand, M. Cinchetti, and G. Malinowski *et al.*, "Engineered materials for all-optical helicity-dependent magnetic switching," Nat. Mater. **13**, 286 (2014).

[10] C. Y. Fong, J. E. Pask, and L. H. Yang, *Half-Metallic Materials and Their Properties*, Materials for Engineering, Vol. 2 (World Scientific Publishing Co, Singapore, 2007).

[11] M. Venkatesan, "Half-metals," in *Handbook of Magnetism and Advanced Magnetic Materials*, Vol. 4, edited by H. Kronmuller and S. Parkin (John Wiley & Sons, Hoboken, 2007) p. 2133.

[12] M. I. Katsnelson, V. Yu. Irkhin, L. Chioncel, A. I. Lichtenstein, and R. A. de Groot, "Half-metallic ferromagnets: From band structure to many-body effects," Rev. Mod. Phys. **80**, 315 (2008).

[13] C. Felser and G. H. Fecher, eds., *Spintronics: From Materials to Devices* (Springer, Dordrecht, 2013).

[14] S. Sugahara, Y. Takamura, Y. Shuto, and S. Yamamoto, "Field effect spin transistors," in *Handbook of Spintronics*, Vol. 2, edited by Y. Xu, D. Awschalom, and J. Nitta (Springer Science+Business Media, Dordrecht, 2016) Chap. 31, p. 1243.

[15] Qiang Zhang, A. V. Nurmikko, G. X. Miao, G. Xiao, and A. Gupta, "Ultrafast spin-dynamics in half-metallic CrO_2 thin films," Phys. Rev. B **74**, 061141 (2006).

[16] G. M. Müller, J. Walowski, M. Djordjevic, G.-X. Miao, A. Gupta, A. V. Ramos, K. Gehrke, V. Moshnyaga, K. Samwer, and J. Schmalhorst *et al.*, "Spin polarization

in half-metals probed by femtosecond spin excitation," Nat. Mater. **8**, 56 (2008).

[17] D. Steil, S. Alebrand, T. Roth, M. Krauß, T. Kubota, M. Oogane, Y. Ando, H. C. Schneider, M. Aeschlimann, and M. Cinchetti, "Band-structure-dependent demagnetization in the Heusler alloy $Co_2Mn_{1-x}Fe_xSi$," Phys. Rev. Lett. **105**, 217202 (2010).

[18] S. Kaltenborn and H. C. Schneider, "Spin-dependent lifetimes and nondegenerate spin-orbit driven hybridization points in Heusler compounds," Phys. Rev. B **89**, 115127 (2014).

[19] M. Krauß, T. Roth, S. Alebrand, D. Steil, M. Cinchetti, M. Aeschlimann, and H. C. Schneider, "Ultrafast demagnetization of ferromagnetic transition metals: The role of the Coulomb interaction," Phys. Rev. B **80**, 180407 (2009).

[20] S. Eich, M. Plötzing, M. Rollinger, S. Emmerich, R. Adam, C. Chen, H. C. Kapteyn, M. M. Murnane, L. Plucinski, and D. Steil *et al.*, "Band structure evolution during the ultrafast ferromagnetic-paramagnetic phase transition in cobalt," Sci. Adv. **3**, e1602094 (2017).

[21] I. L. M. Locht, I. Di Marco, S. Garnerone, A. Delin, and M. Battiato, "Ultrafast magnetization dynamics: Microscopic electronic configurations and ultrafast spectroscopy," Phys. Rev. B **92**, 064403 (2015).

[22] B. S. D. Ch. S. Varaprasad, A. Rajanikanth, Y. K. Takahashi, and K. Hono, "Enhanced spin polarization of Co_2MnGe Heusler alloy by substitution of Ga for Ge," Appl. Phys. Express **3**, 023002 (2010).

[23] G. T. Woods, R. J. Soulen, I. Mazin, B. Nadgorny, M. S. Osofsky, J. Sanders, H. Srikanth, W. F. Egelhoff, and R. Datla, "Analysis of point-contact Andreev reflection spectra in spin polarization measurements," Phys. Rev. B **70**, 054416 (2004).

[24] E. A. Seddon, "Spin-resolved valence photoemission," in *Handbook of Spintronics*, Vol. 1, edited by Y. Xu, D. Awschalom, and J. Nitta (Springer Science+Business Media, Dordrecht, 2016) Chap. 22, p. 831.

[25] M. Jourdan, J. Minár, J. Braun, A. Kronenberg, S. Chadov, B. Balke, A. Gloskovskii, M. Kolbe, H. J. Elmers, and G. Schönhense *et al.*, "Direct observation of half-metallicity in the Heusler compound Co_2MnSi," Nat. Commun. **5**, 3974 (2014).

[26] Yu. S. Dedkov, U. Rüdiger, and G. Güntherodt, "Evidence for the half-metallic ferromagnetic state of Fe_3O_4 by spin-resolved photoelectron spectroscopy," Phys. Rev. B **65**, 064417 (2002); J. G. Tobin, S. A. Morton, S. W. Yu, G. D. Waddill, I. K. Schuller, and S. A. Chambers, "Spin resolved photoelectron spectroscopy of Fe_3O_4: the case against half-metallicity," J. Phys.: Condens. Matter **19**, 315218 (2007); M. Fonin, Yu. S. Dedkov, R. Pentcheva, U. Rüdiger, and G. Güntherodt, "Spin-resolved photoelectron spectroscopy of Fe_3O_4–revisited," *ibid.* **20**, 142201 (2008).

[27] W. Wang, J.-M. Mariot, M. C. Richter, O. Heckmann, W. Ndiaye, P. De Padova, A. Taleb-Ibrahimi, P. Le Fèvre, F. Bertran, and F. Bondino *et al.*, "Fe t_{2g} band dispersion and spin polarization in thin films of $Fe_3O_4(0\,0\,1)$/MgO$(0\,0\,1)$: Half-metallicity of magnetite revisited," Phys. Rev. B **87**, 085118 (2013), and the references cited therein.

[28] B. Rethfeld, A. Kaiser, M. Vicanek, and G. Simon, "Ultrafast dynamics of nonequilibrium electrons in metals under femtosecond laser irradiation," Phys. Rev. B **65**, 214303 (2002).

[29] H. Ebert, D. Ködderitzsch, and J. Minár, "Calculating condensed matter properties using the KKR-Green's function method–recent developments and applications," Rep. Prog. Phys. **74**, 096501 (2011).

[30] Z. Zhang and S. Satpathy, "Electron states, magnetism, and the Verwey transition in magnetite," Phys. Rev. B **44**, 13319 (1991).

[31] M. Fonin, R. Pentcheva, Yu. S. Dedkov, M. Sperlich, D. V. Vyalikh, M. Scheffler, U. Rüdiger, and G. Güntherodt, "Surface electronic structure of the $Fe_3O_4(1\,0\,0)$: Evidence of a half-metal to metal transition," Phys. Rev. B **72**, 104436 (2005).

[32] C. M. Cacho, S. Vlaic, M. Malvestuto, B. Ressel, E. A. Seddon, and F. Parmigiani, "Absolute spin calibration of an electron spin polarimeter by spin-resolved photoemission from the Au$(1\,1\,1)$ surface states," Rev. Sci. Instrum. **80**, 043904 (2009).

[33] K. M. Shen, F. Ronning, W. Meevasana, D. H. Lu, N. J. C. Ingle, F. Baumberger, W. S. Lee, L. L. Miller, Y. Kohsaka, and M. Azuma *et al.*, "Angle-resolved photoemission studies of lattice polaron formation in the cuprate $Ca_2CuO_2Cl_2$," Phys. Rev. B **75**, 075115 (2007).

[34] D. Ihle and B. Lorenz, "Small-polaron conduction and short-range order in Fe_3O_4," J. Phys. C: Solid State Phys. **19**, 5239 (1986).

[35] J. Braun, "The theory of angle-resolved ultraviolet photoemission and its applications to ordered materials," Rep. Prog. Phys. **59**, 1267 (1996).

[36] J. Minár, J. Braun, S. Mankovsky, and H. Ebert, "Calculation of angle-resolved photo emission spectra within the one-step model of photo emission–Recent developments," J. Electron Spectrosc. Relat. Phenom. **184**, 91 (2011).

[37] J. Braun, K. Miyamoto, A. Kimura, T. Okuda, M. Donath, H. Ebert, and J. Minár, "Exceptional behavior of d-like surface resonances on W$(1\,1\,0)$: the one-step model in its density matrix formulation," New J. Phys. **16**, 015005 (2014).